Journal of Power Sources 239 (2013) 253–264

Contents lists available at SciVerse ScienceDirect

Journal of Power Sources

journal homepage: www.elsevier.com/locate/jpowsour

Prognostics of lithium-ion batteries based on relevance vectors and a conditional three-parameter capacity degradation model

Dong Wang [a], Qiang Miao [b,*], Michael Pecht [c]

[a] Department of Systems Engineering & Engineering Management, City University of Hong Kong, Tat Chee Avenue, Kowloon, Hong Kong, China
[b] School of Mechanical, Electronic and Industrial Engineering, University of Electronic Science and Technology of China, Chengdu, Sichuan 611731, China
[c] Center for Advanced Life Cycle Engineering (CALCE), University of Maryland, College Park, MD 20742, USA

HIGHLIGHTS

- Capacity degradation data are fitted by relevance vector machine.
- Relevance vectors are used to find representative training vectors.
- Representative training vectors are fitted by a conditional three-parameter capacity degradation model.
- The developed model consists of an exponential function and a power function.
- The remaining useful life of lithium-ion batteries is estimated.

ARTICLE INFO

Article history:
Received 16 November 2012
Received in revised form
21 March 2013
Accepted 23 March 2013
Available online 2 April 2013

Keywords:
Lithium-ion batteries
State of health
Remaining useful life
Relevance vector machine
Battery capacity degradation model

ABSTRACT

Lithium-ion batteries are widely used as power sources in commercial products, such as laptops, electric vehicles (EVs) and unmanned aerial vehicles (UAVs). In order to ensure a continuous power supply, the functionality and reliability of lithium-ion batteries have received considerable attention. In this paper, a battery capacity prognostic method is developed to estimate the remaining useful life of lithium-ion batteries. This capacity prognostic method consists of a relevance vector machine and a conditional three-parameter capacity degradation model. The relevance vector machine is used to derive the relevance vectors that can be used to find the representative training vectors containing the cycles of the relevance vectors and the predictive values at the cycles of the relevance vectors. The conditional three-parameter capacity degradation model is developed to fit the predictive values at the cycles of the relevance vectors. Extrapolation of the conditional three-parameter capacity degradation model to a failure threshold is used to estimate the remaining useful life of lithium-ion batteries. Three instance studies were conducted to validate the developed method. The results show that the developed method is able to predict the future health condition of lithium-ion batteries.

1. Introduction

Prognostics is an enabling discipline that predicts the time when a component or system will no longer satisfy its functionality requirement in its actual life cycle conditions [1–4]. It estimates the remaining useful life of the component or system [5], where remaining useful life (RUL) [6] is defined as the period from the current time until the system or component fails. Estimation of the RUL is used to conduct maintenance activities, provide spare parts in a timely manner, and prevent accidents.

In recent years, lithium-ion batteries have become the most common power supply for providing portable electronics and electric vehicles (EVs) with electric energy [7]. However, lithium-ion battery functionality gradually deteriorates over time. Failures of lithium-ion batteries result in economic and operational losses and can have catastrophic consequences. In order to evaluate the performance of a lithium-ion battery, state of charge (SOC) and state of health (SOH) estimation techniques are often implemented in lithium-ion battery management systems (BMSs) [7]. SOC is the percentage of the remaining charge to the battery's maximum capacity until the lithium-ion battery needs to be recharged. SOH describes the physical health condition of a battery compared to a fresh battery. The gradual decrease in the capacity of lithium-ion batteries is a health indicator that tracks the degradation of lithium-ion batteries. Lithium-ion battery failures occur when the

* Corresponding author.
E-mail addresses: wangdonguestc@yahoo.cn (D. Wang), mqiang@uestc.edu.cn (Q. Miao), pecht@calce.umd.edu (M. Pecht).

0378-7753/$ – see front matter © 2013 Elsevier B.V. All rights reserved.
http://dx.doi.org/10.1016/j.jpowsour.2013.03.129

capacity degradation data of the lithium-ion battery drops below some percentage of its nominal capacity [8]. The failure threshold is recommended to be around 80% of the rated value because the capacity degradation data exhibit a trend with exponential decay after crossing the 80% threshold [9]. Therefore, at the exponential decay, lithium-ion batteries become unreliable and should be replaced.

Yoshida et al. [10] investigated the capacity loss mechanism of large capacity lithium-ion cells for satellite application and developed a simple life estimation model to fit the capacity loss data. In their subsequent work [11], they revised their previously developed model by considering solid electrolyte interface growth blocking mechanism. The results showed that the revised model can be used to better fit ten-year long-term capacity loss data. Burgess [12] divided the float service life of a battery into two phases. During the first phase, the capacity loss was small. The capacity loss increased once the second phase began. A Kalman filter was applied to estimate the remaining float service life of a valve-regulated lead acid battery once the second phase began. However, the battery capacity fade in the second phase was so short that an early failure alarm could not be triggered by this approach. He et al. [13] developed a lithium-ion battery prognostic method by combining Dempster–Shafer theory (DST) and the Bayesian Monte Carlo (BMC) method. In their research, the sum of two exponential functions was developed as a capacity degradation model, and DST was employed to estimate the initial values of this model. BMC was then adopted to infer the RUL. The advantage of this approach was that it was capable of providing an RUL prediction early in the battery life. However, this method needed historical samples to provide initial model parameters across the population of batteries.

Relevance vector machines (RVMs) [14] are gaining attention in prognostics. An RVM offers good generalization performance in regression and the sparse inferred predictors which are significant predictors corresponding to a few non-zero weight parameters used in a regression function. Saha et al. [15,16] employed a relevance vector machine in a regression to fit the capacity degradation data of lithium-ion batteries. They then used several different particle filters, such as a standard particle filter and a Rao-Blackwellized particle filter, to predict the RUL of the batteries. Their RVM and particle filter framework have been experimentally proven to have advantages, such as reducing the prediction uncertainty, over autoregressive integrated moving average and extended Kalman filtering [17]. Widodo et al. [18] employed sample entropy as a battery health indicator. A support vector machine and a RVM were used to predict the battery health condition. The results showed that a relevance vector machine that is integrated with sample entropy handles prediction uncertainty better than a support vector machine with the sample entropy. Caesarendra et al. [19] used kurtosis, which was the fourth standardized moment, to measure the peakedness of the non-stationary transient signals caused by bearing localized faults and then employed logistic regression, which is a regression analysis method used for quantitatively predicting a categorical variable based on one or more predictor variables, to transform the kurtosis of bearing vibration degradation signals into bearing failure probability. The inputs and target vectors used for training RVM were kurtosis and bearing failure probability, respectively. Then, the trained RVM was employed to track the bearing failure probability of unknown inputs. Maio et al. [20] combined a relevance vector machine and an exponential function to estimate the remaining useful life of bearings. Based on a similar idea, Zio and Maio [21] employed a relevance vector machine to find the most representative relevance vectors to fit a crack growth model for predicting remaining useful life.

In this paper, a relevance vector machine is applied to get the relevance vectors used for finding the representative training vectors. A comparison is done to show that the four parameters of the capacity degradation model in Ref. [13] cannot be uniquely determined with the representative training vectors. In order to obtain unique degradation model parameters, a conditional three-parameter capacity degradation model is developed to fit the representative training vectors. Extrapolation of the conditional three-parameter capacity degradation model to a failure threshold is used to estimate the remaining useful life of lithium-ion batteries.

The rest of this paper is organized as follows. In Section 2, the relevance vector machine is introduced. The battery prognostic method is developed in Section 3. Three instances are investigated in Section 4 to validate the developed method for estimating the remaining useful life of lithium-ion batteries. Conclusions are discussed in Section 5.

2. Brief introduction of relevance vector machine

This section introduces the relevant vector machine that is used in this research. The general regression problem is discussed, and the relevant vector machine and sparse Bayesian learning are presented.

2.1. General regression problem

Given some target measurements $\mathbf{y} = (y_1,y_2,\ldots,y_N)^T$ and some inputs $\mathbf{x} = (x_1,x_2,\ldots,x_N)$, the general regression relationship between the target and input vectors can be described by a model $f(x_i)$ with the addition of noise ε_i [22]:

$$y_i = f(x_i) + \varepsilon_i, i = 1,2,\ldots,N, \tag{1}$$

where $f(x_i)$ is a linear combination of some known basis functions $\phi_j(x_i)$. The mathematical formula of $f(x_i)$ is given as:

$$f(x_i) = \sum_{j=1}^{M} w_j\phi_j(x_i) = \phi(x_i)\mathbf{w}, \tag{2}$$

where $\mathbf{w} = (w_1,w_2,\ldots,w_M)^T$ is a weight vector, and $\phi(x_i) = (\phi_1(x_i),\phi_2(x_i),\ldots,\phi_M(x_i))$. The matrix form of Equation (1) is written as:

$$\mathbf{y} = \overline{\mathbf{\Phi}}\mathbf{w} + \boldsymbol{\varepsilon}, \tag{3}$$

where $\mathbf{\Phi}$ is an $N \times M$ design matrix, whose j-th column consists of N basis functions $\phi_j(x_i), i = 1,2,\ldots,N$, and $\boldsymbol{\varepsilon}$ is a noise vector. Assuming that each element of the noise vector is subject to the independent Gaussian distribution with zero mean and variance σ^2, the likelihood of the complete training data set and the least square estimate $\mathbf{w}_{LS}$ for the weight vector are given by[22]:

$$p\left(\mathbf{y}\middle|\mathbf{w},\sigma^2\right) = \left(2\pi\sigma^2\right)^{-N/2}\exp\left\{-\frac{1}{2\sigma^2}\left\|\mathbf{t} - \overline{\mathbf{\Phi}}\mathbf{w}\right\|^2\right\} \tag{4}$$

$$\mathbf{w}_{LS} = \arg\min_{w}\left(\left\|t - \overline{\mathbf{\Phi}}\mathbf{w}\right\|^2\right) = \left(\overline{\mathbf{\Phi}}^T\overline{\mathbf{\Phi}}\right)^{-1}\overline{\mathbf{\Phi}}^T\mathbf{y} \tag{5}$$

It should be noted that, in many cases, the matrix $\overline{\mathbf{\Phi}}^T\overline{\mathbf{\Phi}}$ is frequently ill-conditioned, resulting in the estimate $\mathbf{w}_{LS}$ suffering from over-fitting and reducing predictive performance.

2.2. Relevance vector machine and sparse Bayesian learning

Relevance vector machine (RVM) is a special sparse linear model which has a form similar to a support vector machine

(SVM). SVM calculates predictions by using the following function [14]:

$$f(x_i) = \sum_{j=1}^{N} w_j K_j(x_i, x_j) + w_0 = \mathbf{\Phi}(x_i)\mathbf{w} \tag{6}$$

where $K_j(x_i,x_j)$ is a kernel function, $\mathbf{\Phi}(x_i) = [1,K(x_i,x_1),K(x_i,x_2),\ldots,K(x_i,x_N)]$, and $\mathbf{w} = (w_0,w_1,\ldots,w_N)^T$. The relevance vector machine is a Bayesian treatment of Equation (6). The kernel function used in the relevance vector machine does not need to satisfy Mercer's condition. Mercer's condition is used to judge whether a kernel is symmetric positive semi-definite and is the dot product of two mapping functions in some Euclidean space. It can avoid computing the mapping function explicitly and use the kernel function instead [23]. However, in many cases, fulfilling Mercer's condition is mathematically intractable. Because of the distribution assumption of the additive noise mentioned in Section 2.1, the likelihood of the complete training data set is written as:

$$p\left(\mathbf{y}\middle|\mathbf{w},\sigma^2\right) = \left(2\pi\sigma^2\right)^{-N/2}\exp\left\{-\frac{1}{2\sigma^2}\|\mathbf{t}-\mathbf{\Phi}\mathrm{w}\|^2\right\} \tag{7}$$

where $\mathbf{\Phi} = [\phi(x_1),\phi(x_2),\ldots,\phi(x_N)]^T$ is a $N \times (N+1)$ design matrix, and $\phi(x_i) = [1,K(x_i,x_1),K(x_i,x_2),\ldots,K(x_i,x_N)]^T$. In order to avoid the severe over-fitting problem caused by the maximum likelihood estimation of the weight vector, a Bayesian method and imposed additional constraint parameters can be adopted. Define a zero-mean Gaussian prior distribution over w [14]:

$$p(\mathbf{w}|\boldsymbol{\alpha}) = \prod_{i=0}^{N} N\left(w_i|0,\alpha_i^{-1}\right) \tag{8}$$

where $\boldsymbol{\alpha} = (\alpha_0,\alpha_1,\ldots,\alpha_N)$ is a vector consisting of $N+1$ hyperparameters. Moreover, an individual hyperparameter is independently associated with each weight. A Gamma prior distribution is conducted on the hyperparameters and the noise variance σ^2 [14]:

$$p(\boldsymbol{\alpha}) = \prod_{i=0}^{N} \mathrm{Gamma}(\alpha_i|a,b) \tag{9}$$

$$p(\beta) = \mathrm{Gamma}(\beta|c,d) \tag{10}$$

where $\beta \equiv \sigma^{-2}$, and $\mathrm{Gamma}(\alpha_i|a,b) = (\int_0^\infty t^{a-1}e^{-t}\mathrm{d}t)^{-1}b^a\alpha^{a-1}e^{-b\alpha}$. When a, b, c, and d are set to zero, uniform hyperpriors over a logarithmic scale are formed.

Given the above prior assumptions and the training data, the posterior over all unknown parameters is given by Ref. [14]:

$$p\left(\mathbf{w},\boldsymbol{\alpha},\sigma^2|\mathbf{y}\right) = \frac{p(\mathbf{y}|\mathbf{w},\boldsymbol{\alpha},\sigma^2)p(\mathbf{w},\boldsymbol{\alpha},\sigma^2)}{p(\mathbf{y})} \tag{11}$$

The posterior shown in Equation (11) cannot be directly calculated and the integral of the denominator cannot be calculated either. In order to solve this problem, the posterior is reformulated as [14]:

$$p\left(\mathbf{w},\boldsymbol{\alpha},\sigma^2|\mathbf{y}\right) = p\left(\mathbf{w}\middle|\mathbf{y},\boldsymbol{\alpha},\sigma^2\right)p\left(\boldsymbol{\alpha},\sigma^2|\mathbf{y}\right) \tag{12}$$

The posterior distribution over the weight vector is given by [14]:

$$\begin{aligned} p\left(\mathbf{w}\middle|\mathbf{y},\boldsymbol{\alpha},\sigma^2\right) &= \frac{p(\mathbf{y}|\mathbf{w},\sigma^2)p(\mathbf{w}|\boldsymbol{\alpha})}{p(\mathbf{y}|\boldsymbol{\alpha},\sigma^2)} \\ &= (2\pi)^{-(N+1)/2}|\mathbf{\Sigma}|^{-1/2} \\ &\quad\times\exp\left\{\frac{-1}{2}(\mathbf{w}-\mu)^T\mathbf{\Sigma}^{-1}(\mathbf{w}-\mu)\right\} \end{aligned} \tag{13}$$

where $\mathbf{\Sigma} = (\sigma^{-2}\mathbf{\Phi}^T\mathbf{\Phi}+\mathbf{A})^{-1}$, $\boldsymbol{\mu} = \sigma^{-2}\mathbf{\Sigma}\mathbf{\Phi}^T\mathbf{y}$ and $\mathbf{A} = \mathrm{diag}(\alpha_0,\alpha_1,\ldots,\alpha_N)$. The posterior distribution over the weight vector can be analytically calculated, since $p(\mathbf{y}|\boldsymbol{\alpha},\sigma^2) = \int p(\mathbf{y}|\mathbf{w},\sigma^2)p(\mathbf{w}|\boldsymbol{\alpha})\mathrm{d}\mathbf{w}$ is a convolution of Gaussians. The second term on the right of Equation (12) is decomposed into [14]:

$$p\left(\boldsymbol{\alpha},\sigma^2|\mathbf{y}\right) \propto p\left(\mathbf{y}\middle|\boldsymbol{\alpha},\sigma^2\right)p(\boldsymbol{\alpha})p\left(\boldsymbol{\sigma}^2\right) \tag{14}$$

Because of the uniform hyperpriors assumption of $p(\boldsymbol{\alpha})$ and $p(\sigma^2)$, Equation (14) becomes maximizing $p(\mathbf{y}|\boldsymbol{\alpha},\sigma^2)$ with respect to $\boldsymbol{\alpha}$ and β. The formula of the marginal likelihood is given as [14]:

$$\begin{aligned} p\left(\mathbf{y}\middle|\boldsymbol{\alpha},\sigma^2\right) &= (2\pi)^{-N/2}\left|\sigma^2\mathbf{I}+\mathbf{\Phi}A^{-1}\mathbf{\Phi}^T\right|^{-1/2} \\ &\quad\times\exp\left\{-\frac{1}{2}\mathbf{t}^T\left(\sigma^2\mathbf{I}+\mathbf{\Phi}A^{-1}\mathbf{\Phi}^T\right)\mathbf{t}\right\}. \end{aligned} \tag{15}$$

An iterative re-estimation method was introduced in [14] to obtain the values of $\boldsymbol{\alpha}_{\mathrm{MP}}$ and σ^2_{MP} that can maximize Equation (15), because the values of $\boldsymbol{\alpha}_{\mathrm{MP}}$ and σ^2_{MP} cannot be directly derived in closed form. Meanwhile, in practice, many elements of the vector $\boldsymbol{\alpha} = (\alpha_0,\alpha_1,\ldots,\alpha_N)$ tend to infinity during the iterative re-estimation procedure. The posterior distribution over the corresponding weights shown in Equation (13) tend to be subject to a normal distribution, $N(0,0)$. In other words, $p(w_i|\mathbf{y},\boldsymbol{\alpha},\sigma^2)$ is highly concentrated around zero. Additionally, many useless basis functions are pruned from the design matrix $\mathbf{\Phi}$ during the iterative re-estimation procedure. As a result, relevance vectors are those training samples that correspond to the remaining non-zero weights. This definition is analogous to the definition of support vectors. Support vectors correspond to the samples on the margin. At last, given a new input x_* and the values of $\boldsymbol{\alpha}_{\mathrm{MP}}$ and σ^2_{MP}, the predictive distribution over the estimated measurement y_* for the new input x_* is given as [14]:

$$\begin{aligned} p\left(y_*\middle|\mathbf{y},\boldsymbol{\alpha}_{\mathrm{MP}},\sigma^2_{\mathrm{MP}}\right) &= \int p\left(y_*\middle|\mathbf{w},\sigma^2_{\mathrm{MP}}\right)p\left(\mathbf{w}\middle|\mathbf{y},\boldsymbol{\alpha}_{\mathrm{MP}},\sigma^2_{\mathrm{MP}}\right) \\ &= N\left(y_*|f_*,\sigma_*^2\right), \end{aligned} \tag{16}$$

where $f_* = \boldsymbol{\mu}^T\phi(x^*)$ and $\sigma_*^2 = \sigma^2_{MP} + \phi(x_*)^T\mathbf{\Sigma}\phi(x_*)$. From Equation (16), the mean of the normal distribution can be treated as the predictive value for the new input. The confidence of the predictive value is determined by the variance of this normal distribution.

3. Method for the estimation of remaining useful life of lithium-ion batteries

When a battery ages over time, its maximum capacity degrades to zero, indicating the deterioration of battery health. Estimation of the remaining maximum capacity ensures the reliability of a battery for providing continuous power supplies to electronic equipment. Battery failure can be considered to occur once the maximum capacity of the battery drops to 80% of its nominal value. Here, 80% is one of the typical examples suggested by reference [9] to determine a specified failure threshold. In this paper, a battery capacity prognostic method is developed to estimate the remaining useful life of lithium-ion batteries. A flowchart of the battery capacity prognostic procedure is shown in Fig. 1. First, the available capacity degradation data are used as the inputs for the developed

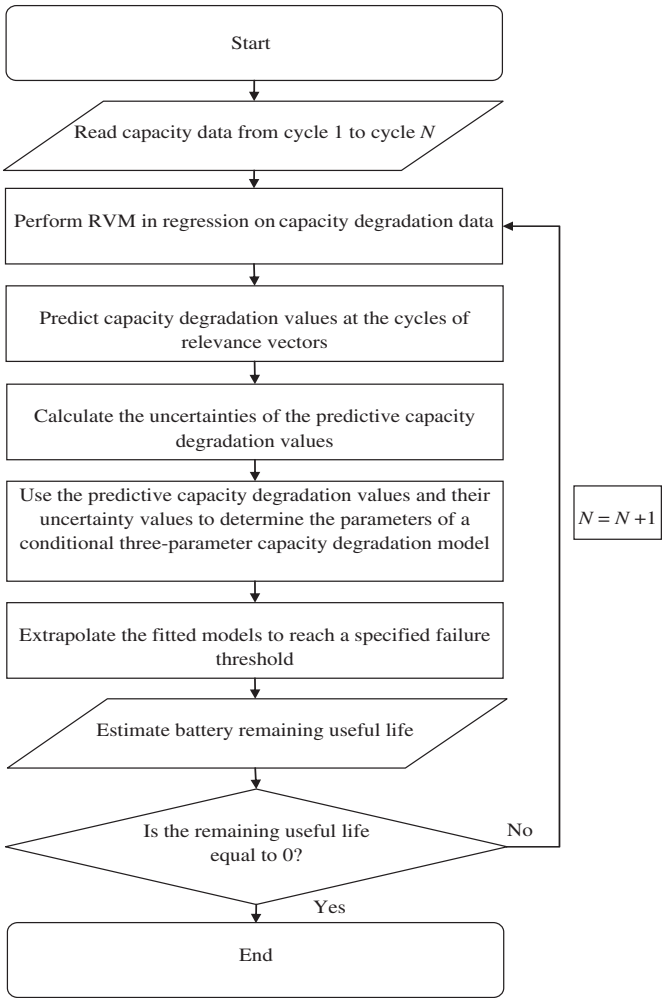

Fig. 1. Procedure for estimating remaining useful life of lithium-ion batteries.

method. Then, RVM is performed on the data for regression analysis. Predictive capacity degradation values and their uncertainties at the cycles of relevance vectors are obtained and they are used to decide the parameters of a conditional three parameter capacity degradation model. Finally, the extrapolation of the established capacity degradation model to a specified failure threshold is used to estimate the outputs of the developed method, namely the remaining useful life of lithium-ion batteries. The details of this procedure are illustrated in the following subsections.

3.1. Capacity degradation data collection

In our research, batteries with graphite anodes and lithium cobalt oxide cathodes were used for testing. The rated capacity was 0.9 Ah. The failure threshold of the batteries was considered to be 0.7 Ah (around 80% of their rated capacity). Multiple charge-discharge tests were performed with an Arbin BT2000 battery testing system under ambient temperature (around 25 °C). The discharge current was 0.45 A. The Coulomb counting method was used to estimate the maximum capacity of the tested batteries. Here, N successive capacity degradation measurements are denoted as $\mathbf{y} = (y_1,y_2,\ldots,y_N)^T$ and their corresponding cycles are $\mathbf{k} = (1,2,\ldots,N)^T$. Therefore, the battery capacity degradation condition can be monitored through the measurements of $\mathbf{y} = (y_1,y_2,\ldots,y_N)^T$.

3.2. Relevance vector selection and the relevance vectors used for finding the representative training vectors

The relevance vector machine described in Section 2.2 is first used to fit the collected lithium-ion battery capacity degradation data $\mathbf{y} = (y_1,y_2,\ldots,y_N)^T$ from cycle 1 to cycle N. The aim of the relevance vector machine in regression is to find a few representative basis functions to derive the prediction model shown in Equation (6) by using sparse Bayesian learning. In our research, a Gaussian basis function is used to create the design matrix $\mathbf{\Phi}$ from Equation (7). The values of $\boldsymbol{\alpha}_{\mathrm{MP}}$ and σ^2_{MP} used for maximizing the marginal likelihood defined in Equation (15) can be indirectly inferred by the iterative re-estimation algorithm mentioned in Section 2.2. Relevance vectors, which are the collected lithium-ion battery capacity degradation data at specific cycles, can be identified through the basis functions with non-zero weights. Here, the relevance vectors are used to find the representative training vectors. Accordingly, the representative training vectors consist of the cycle vectors $\mathbf{l} = (l_1,l_2,\ldots,l_M)^T$ and the predictive values at the cycle vectors. Additionally, the cycles $\mathbf{l} = (l_1,l_2,\ldots,l_M)^T$ correspond to the basis functions in the design matrix $\mathbf{\Phi}$ that have non-zero weights.

According to Equation (16), the predictive mean values at the cycles of $\mathbf{l} = (l_1,l_2,\ldots,l_M)^T$ can be analytically derived as $\tilde{f} = (\boldsymbol{\mu}^T\phi(l_1), \boldsymbol{\mu}^T\phi(l_2), \ldots, \boldsymbol{\mu}^T\phi(l_M))$. Because the predictive distribution over the estimated capacity degradation data is subject to a normal distribution with the variances $\sigma^2_{\mathrm{MP}} + \phi(l_i)^T\Sigma\phi(l_i)$, $i = 1,2,\ldots,M$, the upper and lower confidences of the predictive mean values $\tilde{f} = (\boldsymbol{\mu}^T\phi(l_1), \boldsymbol{\mu}^T\phi(l_2), \ldots, \boldsymbol{\mu}^T\phi(l_M))$ at the cycles of $\mathbf{l} = (l_1,l_2,\ldots,l_M)^T$ can be calculated by the following Equations:

$$\tilde{f}_{\mathrm{upper}} = \left(\boldsymbol{\mu}^T\phi(l_1) + 3 \times \left(\sigma^2_{\mathrm{MP}} + \phi(l_1)^T\Sigma\phi(l_1)\right), \ldots, \boldsymbol{\mu}^T\phi(l_M) + 3 \times \left(\sigma^2_{MP} + \phi(l_M)^T\Sigma\phi(l_M)\right)\right), \tag{17}$$

$$\tilde{f}_{\mathrm{lower}} = \left(\boldsymbol{\mu}^T\phi(l_1) - 3 \times \left(\sigma^2_{\mathrm{MP}} + \phi(l_1)^T\Sigma\phi(l_1)\right), \ldots, \boldsymbol{\mu}^T\phi(l_M) - 3 \times \left(\sigma^2_{\mathrm{MP}} + \phi(l_M)^T\Sigma\phi(l_M)\right)\right). \tag{18}$$

As a result, according to Equations (17) and (18), about 99.7% of the predictive values are within three standard deviations.

3.3. Lithium-ion battery capacity degradation model

A lithium-ion battery capacity degradation model for fitting the predictive mean values of $\tilde{f} = (\boldsymbol{\mu}^T\phi(l_1), \boldsymbol{\mu}^T\phi(l_2), \ldots, \boldsymbol{\mu}^T\phi(l_M))$ at the cycles of $\mathbf{l} = (l_1,l_2,\ldots,l_M)^T$ is developed in this section. In Ref. [24], the sum of exponential functions was employed to track internal impedance. It should be noted that the increase in internal impedance was closely associated with battery capacity degradation. Based on this idea, He et al. [13] experimentally determined that the sum of two exponential functions can be used to fit lithium-ion battery capacity degradation data with different degradation rates. The mathematical formula of the sum of the two exponential functions is given as follows [13]:

$$Q = \eta \times \exp(\iota \times l) + \kappa \times \exp(\lambda \times l), \tag{19}$$

where Q is the capacity of the lithium-ion battery at a specific cycle of l, and η, ι, κ, and λ are four unknown parameters that must be established by a curve fitting method. In this paper, nonlinear least squares regression [25] is employed to estimate the four unknown parameters. In order to alleviate numerical problems with variables

of different scales during the nonlinear least squares regression, the inputs related to the cycles of $\mathbf{l} = (l_1, l_2, \ldots, l_M)^T$ are normalized before the nonlinear least squares regression is performed on the battery capacity degradation data. In order to illustrate the feasibility of Equation (19) for battery capacity degradation data fitting, three battery capacity degradation data, batteries A1, A2 and A3, are processed. The capacity degradation data of lithium-ion batteries A1, A2, and A3, are plotted in Fig. 2(a), (b), and (c), where the dots in each of the subplots show the capacity degradation trends. The batteries have different degradation rates, even though they were tested under the same environment. The fitted curves using Equation (19) are plotted with the thick lines in Fig. 2(a)–(c). Goodness of fit statistics are used to quantify the performance of the model developed by He et al. [13]. The root mean squared error (RMSE), the R^2, and the adjusted R^2 are tabulated in Table 1, where the three statistical values demonstrate that Equation (19) is capable of fitting the lithium-ion battery capacity degradation data. The closer that the value of the RMSE is to 0, the better the performance of the model is. In addition, the closer the values of the R^2 and the adjusted R^2 are to 1, the better the performance of the model.

Equation (19) has four unknown parameters, η, ι, κ, and λ. In our research, it was found that the estimated values of the four parameters used in Equation (19) cannot be uniquely determined if Equation (19) is employed to fit the representative training vectors. In other words, Equation (19) cannot provide a robust curve fitting result given a small amount of capacity degradation training data. For example, after the relevance vector machine is used for the regression of the capacity degradation data from cycle 1 to cycle 108, only 7 relevance vectors are representative of the regression. They are highlighted by the circles in Fig. 3, where the cycles of the representative training vectors are denoted as $\mathbf{l} = (1, 7, 22, 50, 81, 102, 108)^T$. When Equation (19) is employed to fit the same predictive mean values of $\tilde{f} = (\boldsymbol{\mu}^T\phi(1), \boldsymbol{\mu}^T\phi(7), \boldsymbol{\mu}^T\phi(22), \boldsymbol{\mu}^T\phi(50), \boldsymbol{\mu}^T\phi(81), \boldsymbol{\mu}^T\phi(102), \boldsymbol{\mu}^T\phi(108))$ several times, different fitted curves are derived, because the four parameters of Equation (19) cannot be uniquely determined due to the amount of data used. These fitted curves are plotted by thin lines in Fig. 3(a), where these fitted curves have different shapes. Additionally, most of these fitted curves cannot correctly fit the capacity degradation data. From the results illustrated in Fig. 3(a), Equation (19) is not a good candidate for fitting the predictive mean values at the cycles of the representative training vectors because there is only a small amount of representative capacity degradation data used for fitting.

Table 1
Goodness of fit statistics when Equation (19) is used to fit the lithium-ion battery capacity degradation data.

Battery	R^2	Adjusted R^2	RMSE
A1	0.9949	0.9949	0.0042
A2	0.9668	0.9646	0.0116
A3	0.9702	0.9698	0.0088

In order to obtain unique model parameters, it is necessary to simplify Equation (19) without losing its functionality. It is known that one exponential function at zero value can be expanded into the sum of a series of power functions as:

$$\exp(t) = 1 + \frac{t^1}{1!} + \frac{t^2}{2!} + \cdots = \sum_{n=0}^{\infty} \frac{t^n}{n!}, \tag{20}$$

From the representation of the sum of the power functions, one of the two exponential functions in Equation (19) can be

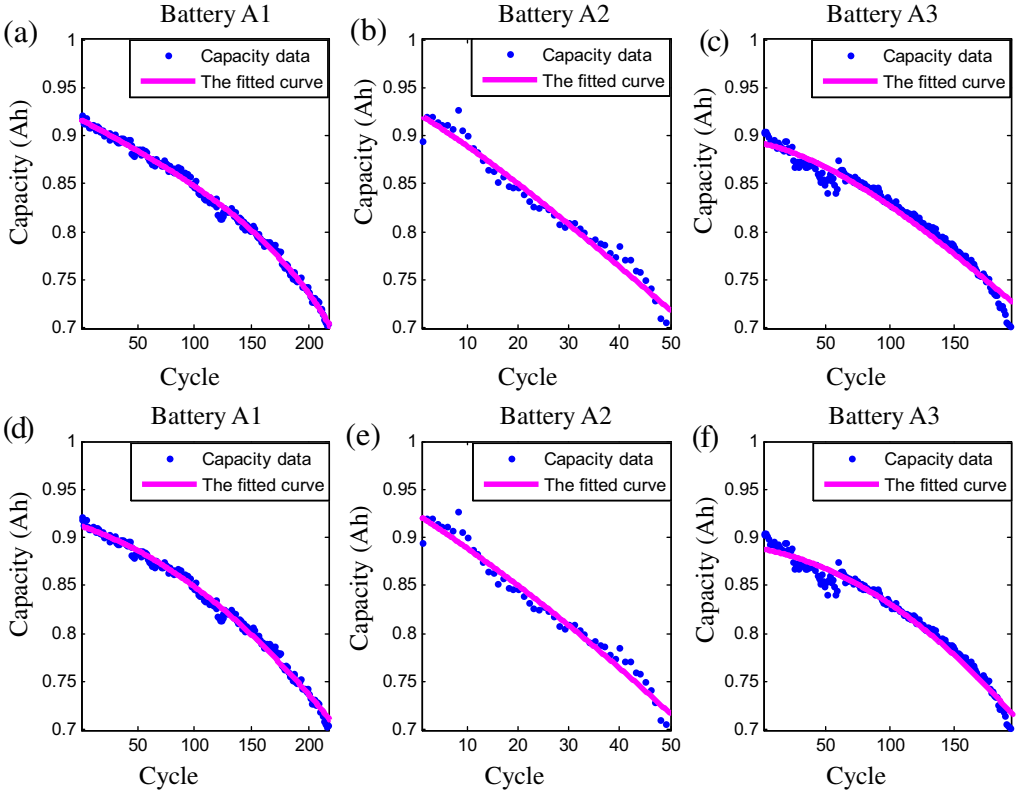

Fig. 2. Comparison of two different models for fitting battery capacity degradation data. Fitted curves using the model developed by He et al. [13] for (a) battery A1, (b) battery A2, (c) battery A3; fitted curves using the model developed in this paper for (d) battery A1, (e) battery A2, (f) battery A3.

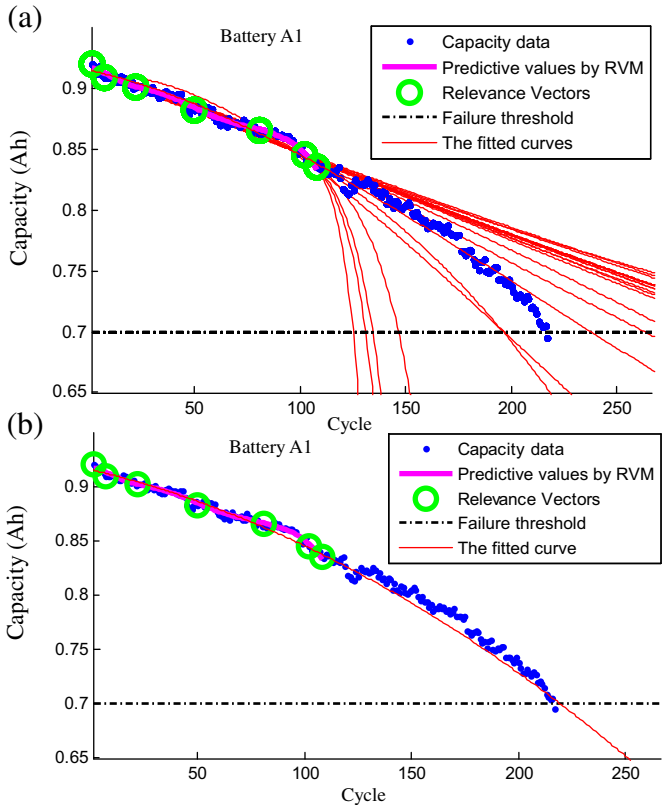

Fig. 3. Fitted curves using the predictive values at the cycles of the representative training vectors with (a) the empirical capacity degradation model developed by He et al. [13]; and (b) the conditional three-parameter capacity degradation model developed in this paper (Note: the capacity degradation data from cycle 1 to cycle 108 are used to find the representative training vectors).

approximately replaced by a power function. Then, a conditional three-parameter capacity degradation model is derived as:

$$Q = \eta \times \exp(\iota \times l) + \kappa \times l^{g}, \tag{21}$$

where g is an integer variable that can be empirically determined by observing the capacity degradation rate. If the capacity degradation trend drops quickly, a large integer value, such as 4, should be used. Otherwise, a small integer value, such as 2, should be taken. The selection of parameter g will be illustrated in Section 4.1. Once the integer variable is determined a priori, only three parameters are left in Equation (21). Therefore, Equation (21) is named the conditional three-parameter capacity degradation model. In other words, such a developed capacity degradation model will have three parameters on the condition that a particular integer variable g is determined by the battery capacity degradation rate. In order to illustrate the performance of Equation (21) on fitting the battery capacity degradation data, the fitted curves obtained by Equation (21) are shown in Fig. 2(d), (e) and (f) with the thin lines. The root mean squared error (RMSE), the R^2, and the adjusted R^2 are tabulated in Table 2, where these values demonstrate that Equation (21) is able to fit the capacity fade data Then, in

Table 2
Goodness of fit statistics when Equation (21) is used to fit the capacity degradation data.

Battery	R^2	Adjusted R^2	RMSE
A1	0.9935	0.9934	0.0048
A2	0.9679	0.9665	0.0113
A3	0.9789	0.9787	0.0074

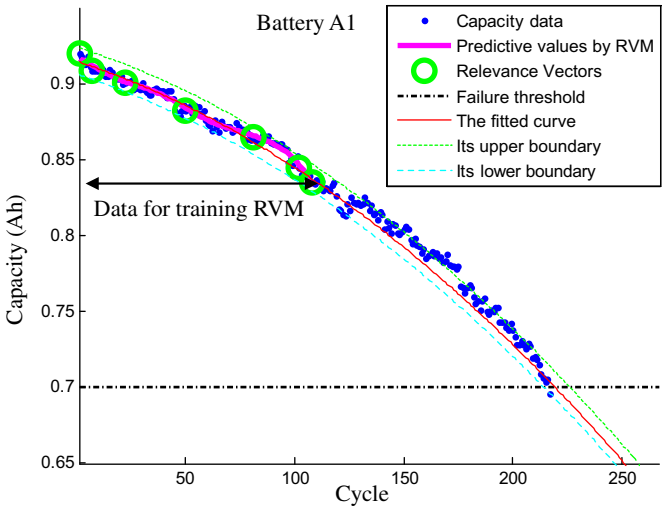

Fig. 4. Predictive results obtained by developed method at inspection cycle 108 for lithium-ion battery A1.

order to compare with Equations (19) and (21) is used to fit the same predictive values obtained by relevance vector machine at cycles $\mathbf{l} = (1, 7, 22, 50, 81, 102, 108)^T$. In Equation (21), g is empirically set to 2 because the drop in the capacity degradation is slow for battery A1, compared to the drops of batteries A2 and A3. The fitted curve is plotted in Fig. 3(b), where it is shown that one unique thin curve is formed. As a result, the developed conditional three-parameter capacity degradation model is better than Equation (19) for capacity degradation data fitting in the case of the relevance vectors used for finding the representative training vectors.

3.4. Remaining useful life estimation and its uncertainties

Given the predictive mean values of $\tilde{f}$ obtained by the relevance vector machine in regression and the prior integer variable, g, the three unknown parameters of the conditional three-parameter capacity degradation model shown in Equation (21) can be uniquely established. Then, the future cycles are input into the conditional three-parameter capacity degradation model with the fixed parameters to predict the future capacity degradation values by

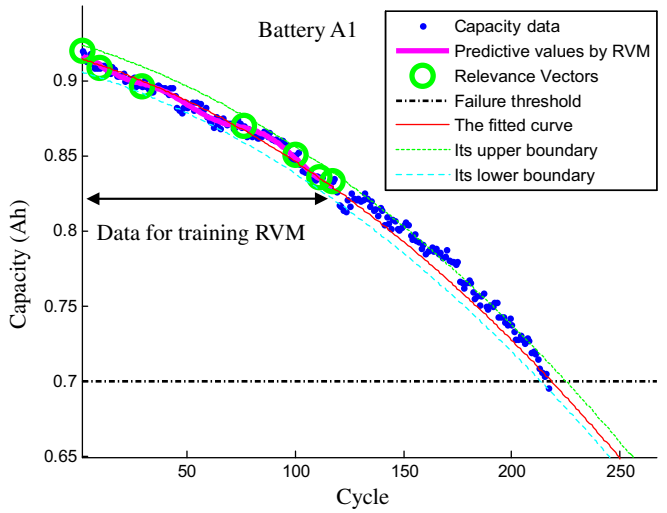

Fig. 5. Predictive results obtained by developed method at inspection cycle 117 for lithium-ion battery A1.

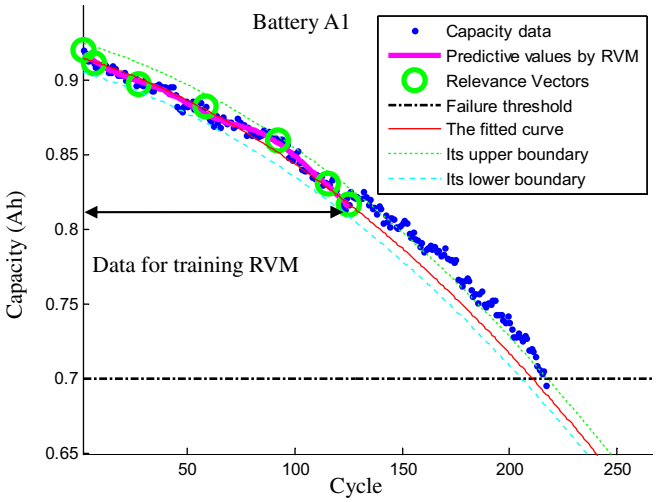

Fig. 6. Predictive results obtained by developed method at inspection cycle 125 for lithium-ion battery A1.

extrapolating the capacity degradation model. Once the predictive future capacity degradation values reach a specified failure threshold, the remaining useful life of the battery at the current cycle N can be estimated by measuring the distance between the cycle N and the cycle N_F at which the predictive future capacity degradation value hits the failure threshold for the first time. Here, the actual failure cycle is denoted as N_A. As a result, the predictive remaining useful life of the battery is given as:

$$\mathrm{RUL}(N) = N_F - N. \tag{22}$$

The same principle can be applied to the upper and lower confidences of the predictive mean values $\tilde{f}_{\mathrm{upper}}$ and $\tilde{f}_{\mathrm{lower}}$, separately, to establish their corresponding capacity degradation models. These models are used to estimate the upper and lower uncertainties of the RUL(N). The predictive failure cycles obtained by the two developed models hitting the failure threshold for the first time are N_F^{upper} and N_F^{lower}. The upper and lower boundaries of the RUL(N) are given as:

$$\mathrm{RUL}_{\mathrm{upper}}(N) = N_F^{\mathrm{upper}} - N, \tag{23}$$

$$\mathrm{RUL}_{\mathrm{lower}}(N) = N_F^{\mathrm{lower}} - N. \tag{24}$$

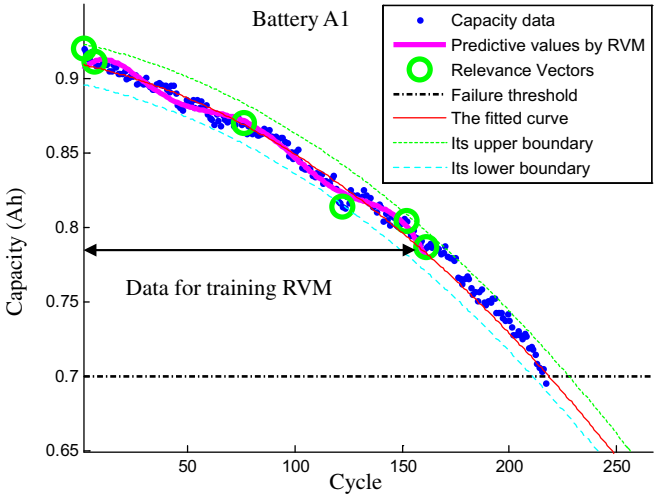

Fig. 7. Predictive results obtained by developed method at inspection cycle 161 for lithium-ion battery A1.

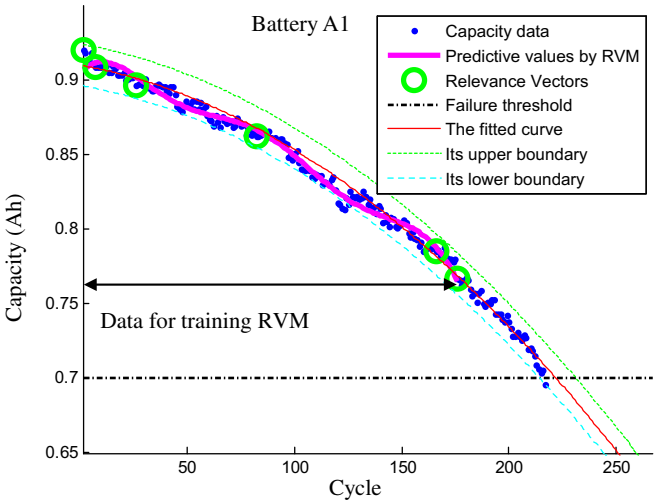

Fig. 8. Predictive results obtained by developed method at inspection cycle 176 for lithium-ion battery A1.

Consequently, by combining Equations (23) and (24), the true value of the RUL(N) will be held by a 99.7% confidence interval $[\mathrm{RUL}_{\mathrm{lower}}(N), \mathrm{RUL}_{\mathrm{upper}}(N)] = [N_F^{\mathrm{lower}} - N, N_F^{\mathrm{upper}} - N]$.

In order to illustrate the accuracy of the developed method, absolute prediction error analysis is used. Its mathematical definition is given as follows:

$$\Delta(N) = |\mathrm{RUL}(N) - \mathrm{RUL}_{\mathrm{True}}(N)|, \tag{25}$$

where $\mathrm{RUL}_{\mathrm{True}}(N)$ is the true RUL at inspection cycle N.

If the remaining useful life is not equal to 0, cycle N is increased by 1 and the new measured capacity degradation value is appended to the vector of $\mathbf{y} = (y_1, y_2, \ldots, y_N)^T$ to form a new vector $\mathbf{y} = (y_1, y_2, \ldots, y_N, y_{N+1})^T$. Then, the above procedure is repeated. Otherwise, the estimation procedure of remaining useful life is terminated.

4. Validation of the developed method

4.1. Instance study 1

In the first instance study, the lithium-ion battery A1 mentioned in Section 3 is investigated. The developed battery capacity

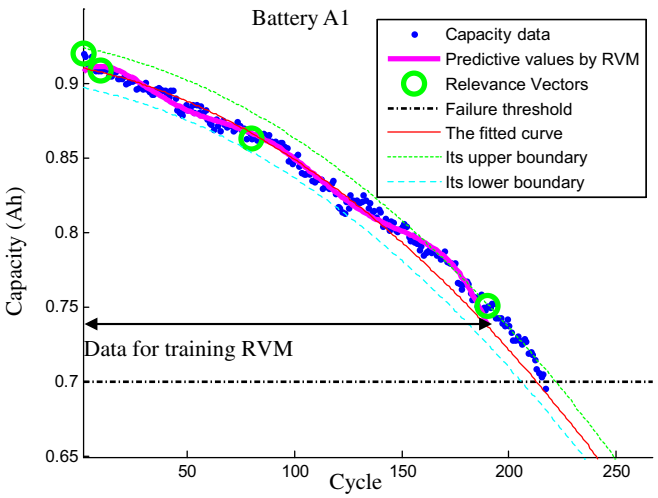

Fig. 9. Predictive results obtained by developed method at inspection cycle 190 for lithium-ion battery A1.

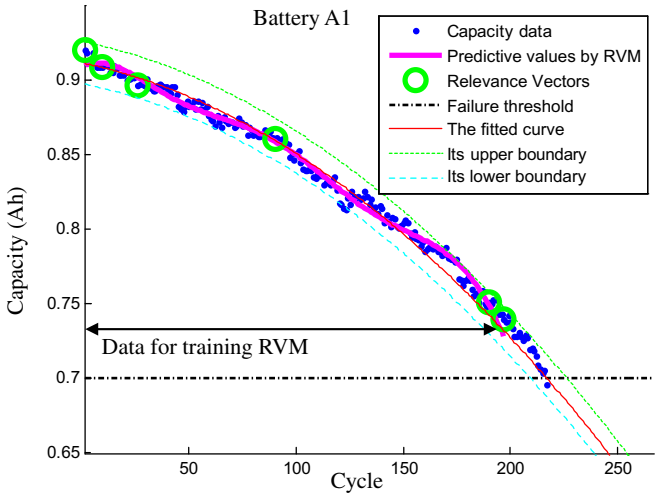

Fig. 10. Predictive results obtained by developed method at inspection cycle 197 for lithium-ion battery A1.

prognostic method is applied to the A1 battery capacity degradation data plotted with dots in Figs. 4–10. Estimations of the remaining useful life of the lithium-ion battery A1 are calculated at the inspection cycles of 108, 117, 125, 161, 176, 190, and 197. These inspection cycles were randomly chosen. The non-zero weights of the weight vectors **w** obtained by sparse Bayesian learning at these inspection cycles are tabulated in Table 3, where **l** represents the cycles of the representative training vectors. The relevance vectors are highlighted by circles in Figs. 4–10. Battery A1 experienced 8% capacity fade within the first 100 cycles, while battery A2 experienced 14% capacity fade much earlier. Therefore, in the case of battery A1, the integer variable g is empirically chosen as 2 for the developed conditional three-parameter capacity degradation model, while, for battery A2, the integer variable g is empirically chosen as 4. The parameters of the conditional three-parameter capacity degradation model are specified in Table 4, where these values are obtained by fitting the predictive values provided by the relevance vector machine at the cycles of the representative training vectors. Only the predictive values at the cycles of the representative training vectors are used for calculating the parameters of the conditional three-parameter capacity degradation model. The predictive values obtained by the relevance vector machine are described by the thick lines in Figs. 4–10, while the fitted curves of the conditional three-parameter capacity degradation model are shown by the thin lines. From Figs. 4–10, the remaining useful life, uncertainties and absolute prediction errors at the inspection cycles are estimated, and they are tabulated in Table 5, where the results validate the developed battery prognostic method for inferring the remaining useful life of lithium-ion batteries.

Table 3
Weights obtained by sparse Bayesian learning at inspection cycles for the lithium-ion battery A1.

Inspection cycle N	Weights and cycles of representative training vectors							
108	**w**	7.42	−9.53	3.84	−0.86	1.82	−4.44	4.05
	l	1	7	22	50	81	102	108
117	**w**	5.03	−6.03	2.59	−1.72	10.37	−21.24	13.38
	l	1	9	29	76	100	111	117
125	**w**	11.48	−13.58	4.26	−1.62	2.76	−4.69	3.73
	l	1	6	27	58	92	115	125
161	**w**	2.82	−2.11	0.70	0.047	−0.64	1.25	
	l	1	6	76	122	152	161	
176	**w**	3.15	−2.57	0.15	0.70	−0.39	1.03	
	l	1	7	26	82	166	176	
190	**w**	2.84	−2.21	0.75	0.65			
	l	1	9	80	190			
197	**w**	4.86	−5.34	1.30	0.59	−0.0039	0.64	
	l	1	9	26	90	190	197	

Table 4
Parameters of developed capacity degradation model (Equation (21)) at different inspection cycles for lithium-ion battery A1.

Inspection cycle N	η	ι	κ
108	0.885	−0.0362	−0.00529
117	0.878	−0.0425	−0.00693
125	0.880	−0.0451	−0.00819
161	0.861	−0.0672	−0.0169
176	0.873	−0.0657	−0.0211
190	0.876	−0.0744	−0.0277
197	0.864	−0.0854	−0.0280

Table 5
Estimated values of remaining useful life and uncertainties at inspection cycles for lithium-ion battery A1 (Unit: cycle).

Inspection cycle N	RUL(N)	Actual RUL	[$RUL_{lower}(N)$,$RUL_{upper}(N)$]	Absolute prediction error
108	113	109	[107,119]	4
117	103	100	[97,109]	3
125	88	92	[81,94]	4
161	59	56	[51,68]	3
176	48	41	[39,56]	7
190	25	27	[17,33]	2
197	22	20	[13,30]	2

4.2. Instance study 2

In the second instance study, the lithium-ion battery A2 described in Section 3 is investigated. As discussed in Section 4.1, the capacity degradation rate for battery A2 is the fastest among the three investigated batteries. The battery capacity prognostic method is then conducted on the A2 battery capacity degradation data, which are plotted as the dots in Figs. 11–15. The inspection cycles of 31, 35, 39, 44, and 48 are randomly chosen for estimating the remaining useful life of lithium-ion battery A2 because the life span of lithium-ion batteries A1, A2, and A3 are different. These inspection cycles are different from those used in instance study 1

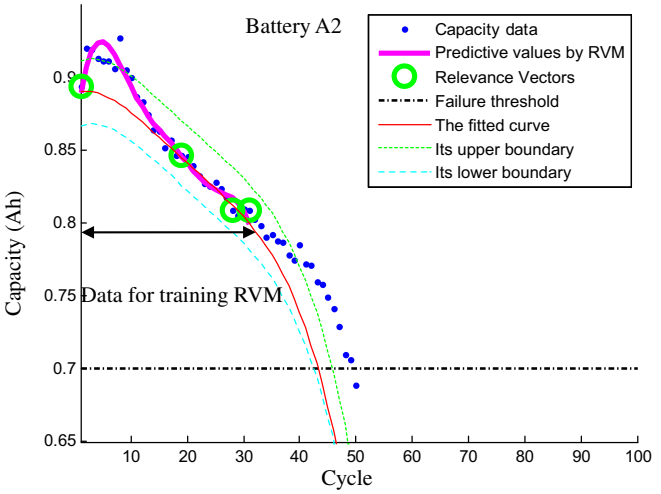

Fig. 11. Predictive results obtained by developed method at inspection cycle 31 for lithium-ion battery A2.

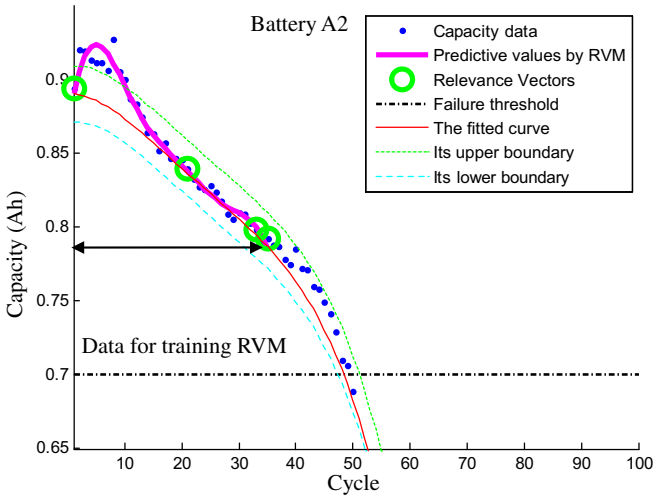

Fig. 12. Predictive results obtained by developed method at inspection cycle 35 for lithium-ion battery A2.

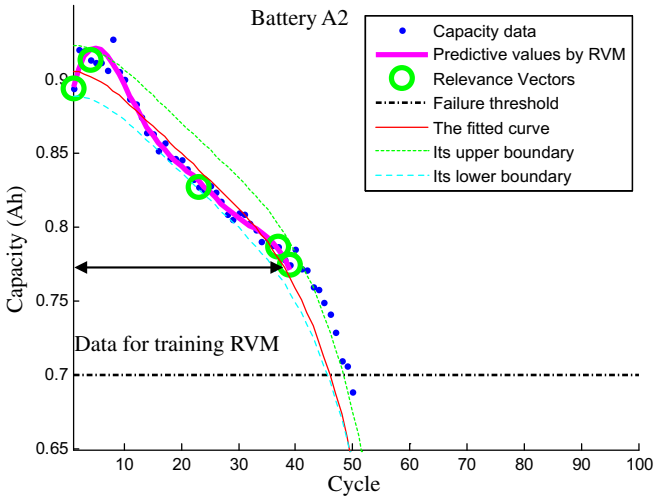

Fig. 13. Predictive results obtained by developed method at inspection cycle 39 for lithium-ion battery A2.

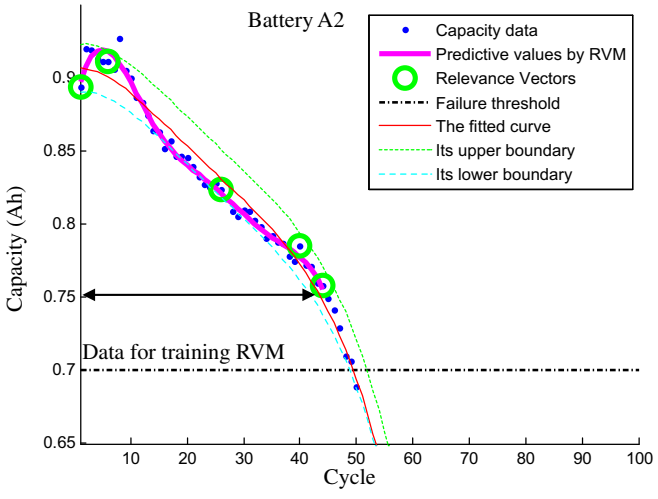

Fig. 14. Predictive results obtained by developed method at inspection cycle 44 for lithium-ion battery A2.

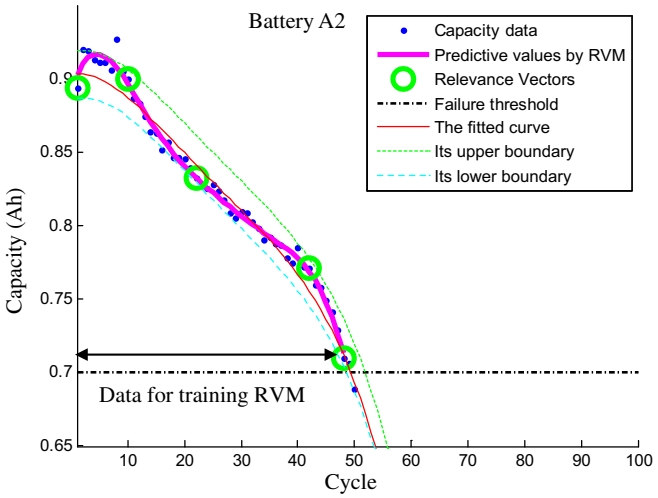

Fig. 15. Predictive results obtained by developed method at inspection cycle 48 for lithium-ion battery A2.

Table 6
Weights obtained by sparse Bayesian learning at different inspection cycles for lithium-ion battery A2.

Inspection cycle N	Weights and cycles of representative training vectors					
31	**w**	0.80	0.79	−1.05	1.48	
	l	1	19	28	31	
35	**w**	0.80	0.71	−1.41	1.90	
	l	1	21	33	35	
39	**w**	0.87	−0.080	0.69	−1.43	1.93
	l	1	4	23	37	39
44	**w**	0.90	−0.10	0.73	−0.88	1.33
	l	1	6	26	40	44
48	**w**	1.02	−0.42	0.72	−0.040	0.64
	l	1	10	22	42	48

Table 7
Parameters of capacity degradation model (Equation (21)) at different inspection cycles for lithium-ion battery A2.

Inspection cycle N	η	ι	κ
31	0.845	−0.0575	−0.00678
35	0.834	−0.0654	−0.00607
39	0.850	−0.078	−0.0140
44	0.844	−0.087	−0.0144
48	0.834	−0.0958	−0.0163

because the degradation rates of battery A1 and battery A2 are different. The non-zero weights of the weight vectors **w** obtained by sparse Bayesian learning at inspection cycles 31, 35, 39, 44, and 48 are tabulated in Table 6, where the vector **l** contains the cycles of the representative training vectors. The relevance vectors are highlighted by the circles in Figs. 11–15. The parameters of the

Table 8
Estimated values of remaining useful life and uncertainties at different inspection cycles for lithium-ion battery A2 (Unit: cycle).

Inspection cycle N	RUL(N)	Actual RUL	[$RUL_{lower}(N)$,$RUL_{upper}(N)$]	Absolute prediction error
31	14	19	[12,15]	5
35	15	15	[13,17]	0
39	9	11	[7,10]	2
44	7	6	[5,8]	1
48	3	2	[1,4]	1

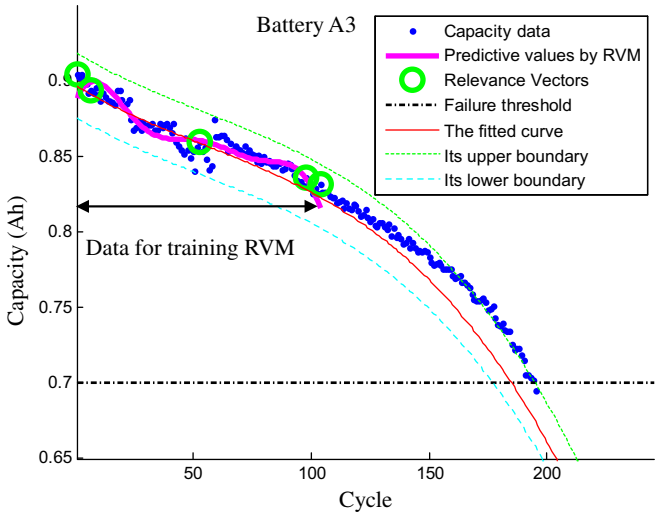

Fig. 16. Predictive results obtained by developed method at inspection cycle 104 for lithium-ion battery A3.

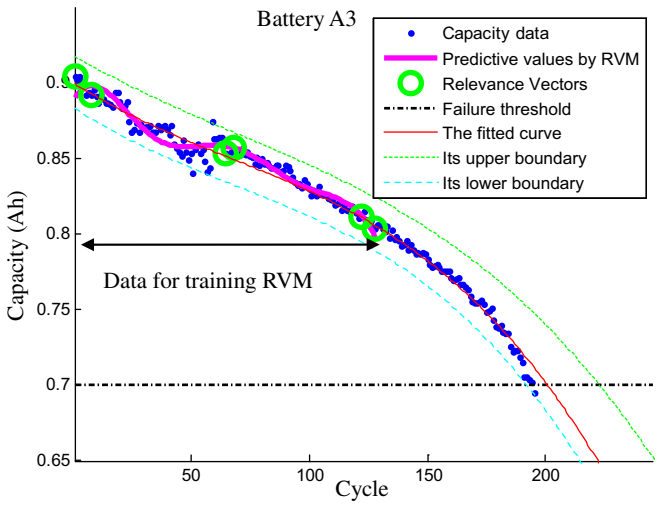

Fig. 17. Predictive results obtained by developed method at inspection cycle 128 for lithium-ion battery A3.

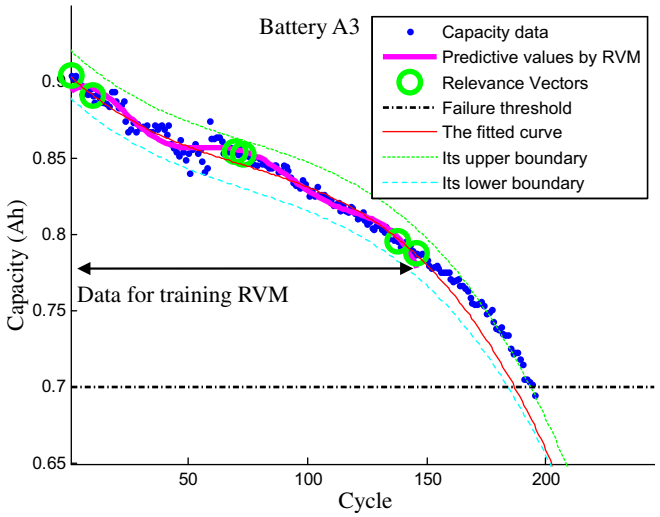

Fig. 18. Predictive results obtained by developed method at inspection cycle 146 for lithium-ion battery A3.

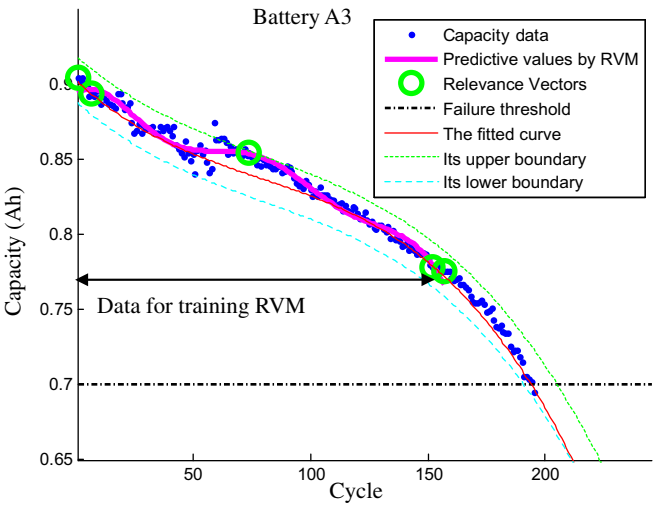

Fig. 19. Predictive results obtained by developed method at inspection cycle 157 for lithium-ion battery A3.

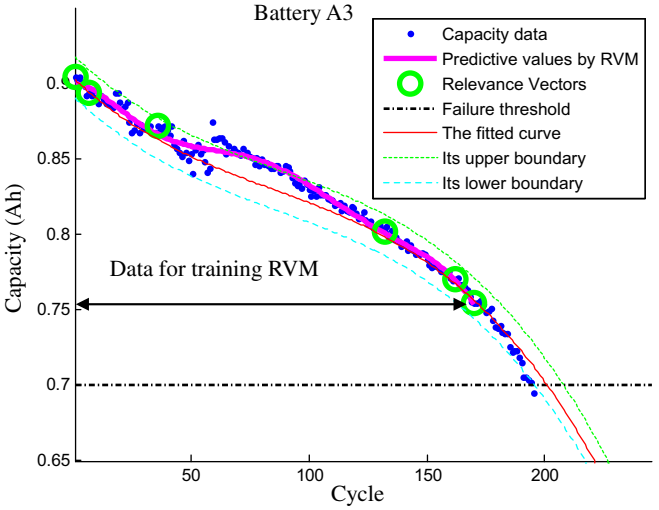

Fig. 20. Predictive results obtained by developed method at inspection cycle 170 for lithium-ion battery A3.

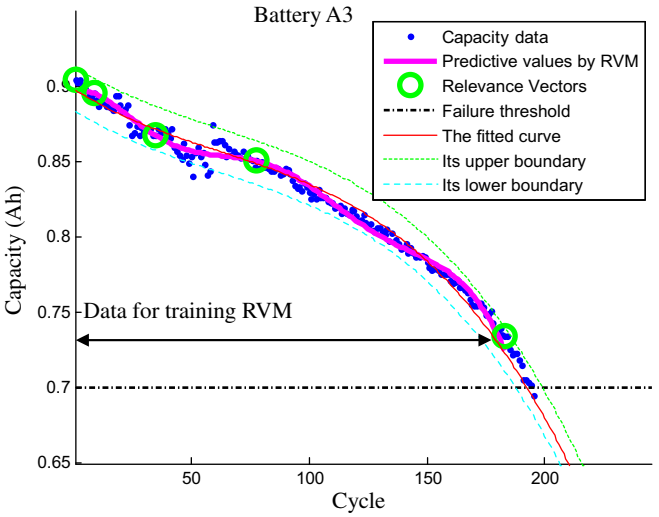

Fig. 21. Predictive results obtained by developed method at inspection cycle 183 for lithium-ion battery A3.

Table 9
Weights obtained by sparse Bayesian learning at different inspection cycles for lithium-ion battery A3.

Inspection cycle N	Weights and cycles of representative training vectors						
104	**w**	1.54	−0.81	0.69	−0.68	1.32	
	l	1	7	53	98	104	
128	**w**	1.63	−0.90	0.39	0.33	−1.04	1.66
	l	1	8	65	68	122	128
146	**w**	1.84	−1.16	0.70	0.034	−0.60	1.23
	l	1	10	70	73	138	146
157	**w**	2.65	−1.96	0.72	−0.85	1.49	
	l	1	7	74	152	157	
170	**w**	7.01	−7.35	1.52	0.97	−3.09	3.07
	l	1	7	36	132	162	170
183	**w**	3.49	−3.06	0.25	0.70	0.64	
	l	1	9	35	78	183	

developed capacity degradation model are tabulated in Table 7. These parameters are calculated by fitting the predictive values estimated by the relevance vector machine only at the cycles of the representative training vectors. The predictive values provided by the relevance vector machine are shown by the thick lines in Figs. 11–15, while the fitted curves of the capacity degradation model are depicted by the thin lines. The remaining useful life, uncertainties and absolute prediction errors at the inspection cycles from these fitted curves are tabulated in Table 8, where the results illustrate that most of the actual battery remaining useful life is covered by the uncertainty intervals of the predicted remaining useful life. Additionally, since more than 31 capacity degradation data is used to train the relevance vector machine and obtain the relevance vectors, the accuracy of battery remaining useful life prediction improves.

4.3. Instance study 3

In the final instance study, lithium-ion battery A3 is investigated. The battery A3 capacity degradation data, plotted with the dots in Figs. 16–21, are analyzed by the battery capacity prognostic method. The inspection cycles of 104, 128, 146, 157, 170, and 183 were randomly chosen. Sparse Bayesian learning is employed to obtain the non-zero weights of the weight vectors **w** at these inspection cycles. The values of the weights are tabulated in Table 9. The relevance vectors are highlighted by the circles in Figs. 16–21. Since the A3 capacity degradation rate is similar to that of battery A1 and slower than that of battery A2, the integer variable g can be chosen as either 2 or 3. The parameters of the conditional three-parameter capacity degradation model obtained by the nonlinear least squares regression are shown in Table 10. It should be noted that the parameter values are obtained by fitting the capacity degradation values predicted by the relevance vector machine at the cycles of the representative training vectors. Only 4 to 6 values at the cycles of the representative training vectors are used for the fitting process. The predictive values obtained by the relevance vector machine at the cycles of the training data are plotted by the thick lines in Figs. 16–21, while the fitted curves of the conditional three-parameter capacity degradation model are depicted by the thin lines. From the fitted curves reaching the failure thresholds in Figs. 16–21, the remaining useful life, uncertainties and absolute prediction errors at the inspection cycles are given in Table 11. The results demonstrate that the developed method is effective in predicting remaining useful life of lithium-ion batteries.

Table 10
Parameters of capacity degradation model (Equation (21)) at different inspection cycles for lithium-ion battery A3.

Inspection cycle N	η	ι	κ
104	0.859	−0.0352	−0.00401
128	0.85	−0.040	−0.0045
146	0.847	−0.0373	−0.0128
157	0.839	−0.0473	−0.0216
170	0.831	−0.0545	−0.0199
183	0.858	−0.0447	−0.0165

Table 11
Estimated values of remaining useful life and uncertainties at different inspection cycles for lithium-ion battery A3 (Unit: cycle).

The inspection cycle of N	RUL(N)	Actual RUL	[$RUL_{lower}(N)$,$RUL_{upper}(N)$]	Absolute prediction error
104	82	91	[73,91]	9
128	74	67	[65,87]	7
146	45	49	[37,48]	4
157	38	38	[35,48]	0
170	33	25	[26,39]	8
183	11	12	[5,17]	1

5. Conclusions

In this paper, a lithium-ion battery capacity prognostic method and a conditional three-parameter capacity degradation model were developed to estimate remaining useful life. First, the battery capacity degradation data from cycle 1 to cycle N was regressed using a relevance vector machine and the relevance vectors were found. The relevance vectors were those capacity degradation training data that corresponded to the non-zero weights for the design matrix. Then, the cycles of the relevance vectors were obtained. The predictive values at the cycles of the representative training vectors were obtained by relevance vector machine prediction. The cycles of the relevance vector with the corresponding predictive formed the representative training vectors. Based on the representative training vectors, the parameters of the developed battery capacity degradation model were calculated by nonlinear least squares regression. Extrapolation of the established capacity degradation model was employed to reach the failure threshold, and the remaining useful life of the lithium-ion batteries was estimated.

To illustrate how the developed battery capacity prognostic method can be used, three instance studies for batteries A1, A2 and A3 were conducted. For battery A1, because about 8% of the maximum capacity of the A1 battery capacity degradation data from cycle 1 to cycle 100 was reduced, g was empirically selected as 2. The absolute prediction errors for the inspection cycles were 4 cycles, 3 cycles, 4 cycles, 3 cycles, 7 cycles, 2 cycles and 2 cycles. For battery A2, since capacity degradation data from cycle 1 to cycle 31 was reduced by about 14% of the maximum capacity, g was empirically chosen as 4. The absolute prediction errors at the inspection cycles were 5 cycles, 0 cycles, 2 cycles, 1 cycle, and 1 cycle. For battery A3, since the A3 capacity degradation rate was similar to that of battery A1 and slower than that of battery A2, g could be chosen as either 2 or 3. The absolute prediction errors for the inspection cycles were 9 cycles, 7 cycles, 5 cycles, 0 cycles, 8 cycles and 1 cycle. As more capacity degradation data were used to train the relevance vector machine and obtain the relevance vectors used for finding the representative training vectors, the accuracy of battery remaining useful life prediction improved.

This paper has four main contributions. First, relevance vectors are used to find the representative training vectors. This step selects significant training vectors and removes most irrelevant and redundant training vectors from the data, thereby improving the performance of RUL prediction. Second, a conditional three-

parameter model for describing lithium-ion battery capacity degradation is developed. The conditional three-parameter capacity degradation model has three parameters given that a particular integer variable, g, is determined by battery capacity degradation rate. Compared with the sum of two exponential functions developed by He et al. [13], the developed model fits capacity degradation data without losing the functionality of the sum of two exponential functions. The results experimentally demonstrate that the developed model can characterize the non-linear relationship between the inspection cycles and the capacity degradation trends. In the case of the representative training vectors used as data for estimating the parameters of lithium-ion battery capacity degradation models, the parameters of the sum of two exponential functions cannot be uniquely determined, while the parameters of the developed conditional three-parameter capacity degradation model can be uniquely decided. Therefore, the developed model is more suitable for battery RUL prediction when the representative training vectors are used as the training capacity data. Third, compared with the model developed by He et al. [13], which needs initial parameters specified by Dempster–Shafer theory or the mean averaging approach, our developed prognostic method does not require specific initial parameters. This means that the initial parameters for our developed model can be randomly chosen. This simplifies the steps for estimation of remaining useful life. Fourth, because of lacking enough historical data to investigate a metric, such as the gradient of capacity fade, an empirical method for the selection of the parameter g is introduced. If the capacity degradation trend drops quickly, a large integer value, such as 4, could be used. Otherwise, a small integer value, such as 2, could be taken.

Acknowledgments

This research was partially supported by the National Natural Science Foundation of China (Grant No. 50905028, 51275554), the Program for New Century Excellent Talents in University (Grant No. NCET-11-0063), and the Zhongshan Science and Technology Project (Grant No. 20123A338). Additionally, we would like to thank the CALCE PHM Group, University of Maryland, for providing the experimental data and suggestions to improve this paper.

References

[1] M. Pecht, Prognostics and Health Management of Electronics, first ed., Wiley-Interscience, London, 2008.
[2] S. Cheng, M.H. Azarian, M. Pecht, Sensors 10 (2010) 5774–5797.
[3] Z.-S. Ye, M. Xie, Y. Shen, L.-C. Tang, Technometrics 54 (2012) 159–168.
[4] D. Wang, Q. Miao, R. Kang, Journal of Sound and Vibration 324 (2009) 1141–1157.
[5] J. Sun, H. Zuo, W. Wang, M.G. Pecht, Mechanical Systems and Signal Processing 28 (2012) 585–596.
[6] X.-S. Si, W. Wang, C.-H. Hu, D.-H. Zhou, European Journal of Operational Research 213 (2011) 1–14.
[7] Y. Xing, E.W.M. Ma, K.L. Tsui, M. Pecht, Energies 4 (2011) 1840–1857.
[8] J. Zhang, J. Lee, Journal of Power Sources 196 (2011) 6007–6014.
[9] M. Dubarry, B.Y. Liaw, Journal of Power Sources 194 (2009) 541–549.
[10] H. Yoshida, N. Imamura, T. Inoue, K. Komada, Electrochemistry 71 (2003) 1018–1024.
[11] H. Yoshida, N. Imamura, T. Inoue, K. Takeda, H. Naito, Electrochemistry 78 (2010) 482–488.
[12] W.L. Burgess, Journal of Power Sources 191 (2009) 16–21.
[13] W. He, N. Williard, M. Osterman, M. Pecht, Journal of Power Sources 196 (2011) 10314–10321.
[14] M.E. Tipping, The Journal of Machine Learning Research 1 (2001) 211–244.
[15] B. Saha, K. Goebel, S. Poll, J. Christophersen, Instrumentation and Measurement, IEEE Transactions on 58 (2009) 291–296.
[16] K. Goebel, B. Saha, A. Saxena, J. Celaya, J. Christophersen, Instrumentation & Measurement Magazine, IEEE 11 (2008) 33–40.
[17] B. Saha, Transactions of the Institute of Measurement and Control 31 (2009) 293–308.
[18] A. Widodo, M.-C. Shim, W. Caesarendra, B.-S. Yang, Expert Systems with Applications 38 (2011) 11763–11769.
[19] W. Caesarendra, A. Widodo, B.-S. Yang, Mechanical Systems and Signal Processing 24 (2010) 1161–1171.
[20] F. Di Maio, K.L. Tsui, E. Zio, Mechanical Systems and Signal Processing 31 (2012) 405–427.
[21] E. Zio, F. Di Maio, Expert Systems with Applications 39 (2012) 10681–10692.
[22] D.G. Tzikas, L. Wei, A. Likas, Y. Yang, P. Galatsanos, University of Ioannina, Ioanni, Greece, Illinois Institute of Technology, Chicago, USA, 2006.
[23] C.J.C. Burges, Data Mining and Knowledge Discovery 2 (1998) 121–167.
[24] M. Ecker, J.B. Gerschler, J. Vogel, S. Käbitz, F. Hust, P. Dechent, D.U. Sauer, Journal of Power Sources 215 (2012) 248–257.
[25] G.A.F. Seber, C.J. Wild, Nonlinear Regression, Wiley-Interscience, New York, 2003.